Role of Dynamic Flexibility in Computing Solvatochromic Properties of Dye−Solvent Systems: *o*-Betaine in Water

N. Arul Murugan* and Hans Ågren

Department of Theoretical Chemistry, School of Biotechnology, Royal Institute of Technology, SE-10691 Stockholm, Sweden

Received: November 4, 2008; Revised Manuscript Received: December 13, 2008

Car−Parrinello molecular dynamics (CPMD) and Car−Parrinello mixed quantum mechanics/classical mechanics (CP-QM/MM) calculations were performed for *o*-betaine (OB) in the gas phase and water as solvent to study the solvent dependence on its molecular properties: geometry, charge distribution, and dipole moment. It is found that the molecular geometry in the gas phase is close to the planar structure, while in the water it is a twisted structure. The calculations clearly show that in both the gas phase and water the OB molecule is highly flexible with a large amplitude for the twist angle motion. The average gas-phase dipole moment for OB doubles in water, something that concords with a strong increase of total charge on phenoxide and pyridinium rings. We also investigated the solvatochromic shift in the $\pi-\pi^*$ and $n-\pi^*$ transitions by carrying out INDO/CIS calculations for the gas-phase and solution-phase configurations obtained from the CPMD and CP-QM/MM calculations with results that are in good agreement with available experimental values (*J. Chem. Soc., Perkin Trans. 2* **1999**, *1*, 713). Our work indicates the importance of allowing full structural and dynamic flexibility of dye−solvent systems in predicting their basic solvatochromic properties.

1. Introduction

Pyridinium *N*-phenolate betaine dyes play an important role in solution chemistry as indicators of the polarity scale of solvents.[1−6] These betaine dyes exhibit an intramolecular charge-transfer absorption band that depends on the solvent polarity.[3] Among these dyes, the 2,6-diphenyl(2,4,6-triphenyl-1-pyridinio) phenolate betaine dye, also called E_T30, has been used as a reference dye to define the solvent polarity scale. The solvatochromic shift of this dye has been calculated in a very large number of solvents as well as binary solvents.[3] The solvent polarity scale includes the contributions from the macroscopic quantities of solvents such as the dielectric constant, permittivity, and refractive index and also effects arising from specific and nonspecific solute−solvent interactions. E_T30 exhibits a strong negative solvatochromism[1] and shows a remarkable solvatochromic shift of 357 nm (9730 cm^{-1}) on going from diethyl ether to water as solvent.[1] The solvatochromic shift increases to 453 nm when the solvent environment for the dye is changed from tetramethylsilane to water; these two solvents represent, in fact, the extremes of the polarity scale.[7] Synthetic and absorption studies have been carried out on unsubstituted pyridiniophenoxide, indicating that the pyridinium *N*-phenolate is the responsible chemical part for the solvatochromic behavior of these dyes.[8]

The solvatochromic shifts in different solvents have been reproduced qualitatively based on ab initio calculations employing the self-consistent reaction field approach.[8] On the basis of these reports many theoretical investigations were carried out on 2- and 4-pyridiniophenoxides to establish relationships between molecular structures and properties such as dipole moments,[8] excitation energies,[9] and hyperpolarizabilities.[10] Interestingly, the twist angle between the two rings and hence the molecular geometry has been reported to be strongly dependent on the nature of the solvents.[11] ZINDO/PCM calculations carried out on E_T30 dye have shown that the twist angle (the dihedral angle between the planes of pyridinium and phenoxide rings; defined as ϕ in Figure 1) increases with the solvent polarity.[11] The twist angle for 2-pyridiniophenoxide (or *o*-betaine) in the gas phase has been reported to be 30°.[11] On the basis of free energy perturbation theory the optimum twist angle has been predicted to be 60° for betaine in water.[12] Recently, sequential Monte-Carlo Quantum mechanics calculations (S-MC/QM) have been reported for *o*-betaine (OB) in water where the solvation structure, dipole moment change, and solvatochromic shift are discussed[13] and the OB solute molecule is treated as a rigid body with a fixed twist angle of 60°. The solvatochromic shift of the $n-\pi^*$ excitation, obtained from INDO/CIS calculations carried out over the simulated trajectory, is 6360 cm^{-1}. The experimental λ_{max} values in water and toluene are, respectively, 378 and 529 nm.[8] The calculated solvatochromic shift for OB from water to toluene solvent is 7552 cm^{-1}. Consequently, the solvatochromic shift in water when compared to the gas phase of OB should be larger than 7552 cm^{-1}. The solvatochromic shift in water when compared to the gas phase has been calculated to be between 6686 and 9212 cm^{-1}, and this has been obtained from interpolation of the absorption data

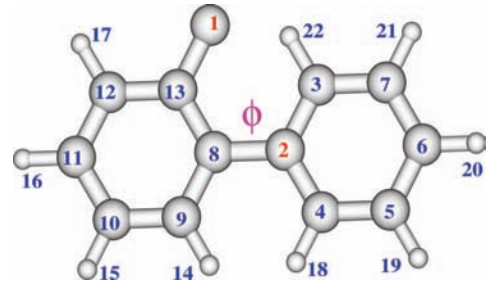

Figure 1. Molecular structure of OB. The twist angle between the phenoxide and pyridinium rings is shown as ϕ in the figure.

* To whom correspondence should be addressed. E-mail: murugan@theochem.kth.se.

10.1021/jp8097395 CCC: $40.75
Published on Web 02/17/2009

of OB in various solvents.[8] Unfortunately, the gas-phase data have been reported with an error bar as large as ±1266 cm^{-1}, which has been attributed to the deviations seen in the experimental data to the fitted regression curve. Thus, the combined S-MC/QM and INDO/CIS calculations seem to reproduce the lower limit of the solvatochromic shift value of OB in water.

The present work generalizes the recent results by exploring the solvatochromic shift values obtained when the solute−solvent interaction is described with a flexible solute molecule. A flexible treatment of OB in water might be important for reproduction of the correct molecular geometry, the correct dipole moment, and the electronic spectra. In order to fulfill these goals we use in this work Car−Parrinello mixed quantum mechanics-molecular mechanics (CP-QM/MM)[14−17] calculations to study OB in water. For comparison with the molecular properties in the gas phase, we also carried out Car−Parrinello molecular dynamics (CPMD)[18] calculations for a single OB molecule. The atomic charges, dipole moments, and molecular geometry were calculated for OB including the full solvent dependence on these properties. Also, the solvation shell structure of OB has been discussed using various radial distribution functions. The electronic spectra have been calculated for the gas-phase trajectory using the INDO/CIS[19] method. Moreover, the electronic spectra for OB in water have been calculated from the CP-QM/MM trajectories by including OB and water molecules up to the third solvation shell. The distribution of peak positions for $\pi-\pi^*$ and $n-\pi^*$ excitations for OB in the gas phase and water has also been predicted.

2. Computational Details

2.1. Car−Parrinello Molecular Dynamics Calculations. A single OB molecule was optimized at the HF level using the 6-31G(d,p) basis set using the Gaussian03 software.[20] The optimized structure along with the GAFF[21] force field has been used to define the OB for initial molecular dynamics calculations. The OB molecule has been solvated with 9832 water molecules in an orthorhombic box with a size of approximately 70.4, 66.7, and 63.7 Å. The water molecules were described using the TIP3P force field[22] and allowed to equilibrate under ambient conditions using molecular dynamics (MD) calculations in an isothermal−isobaric ensemble for a time scale of 100 ps. The MD calculations were carried out using the SANDER module of the Amber8 software.[23] The final configuration was used as the input configuration for the CP-QM/MM calculations. In our present calculations we used the Becke, Lee, Yang, and Parr (BLYP) gradient-corrected functional[24,25] and the Troullier−Martins norm conserving pseudopotentials.[26] Here, the electronic wave function is expanded in a plane wave basis set and the cutoff used was 80 Ry. We used 5 au as the time step for integration of the equation of motion and 600 amu as the fictitious electronic mass. The calculations were carried out in a QM/MM setup,[15−17,27] where the OB molecule is treated at the density functional theory level and the water solvents are treated with a molecular mechanics force field (TIP3P). The QM/MM implementation used here includes the coupling between the QM and the instantaneous electrostatic field arising due to the dynamic MM environment. The interaction between the QM and the MM systems involves electrostatic, short-range repulsion, and long-range dispersion interaction terms (using the empirical van der Waals parameters). In the present QM/MM calculations the polarization effect of the solvent on solute molecule is included. However, the back-polarization effect (due to the solute dipole on solvents) is not included. It is possible to include this effect in the present calculations by selecting solute and solvent molecules in the first solvation shell as the QM part and remaining solvent molecules as the MM part. We, however, still adopted the procedure where only the solute is treated as the QM part and all solvent molecules are treated as the MM part because the betaine−water system has as many as 10−20 water molecules in the first solvation shell. (See Figure 1s and 2s of the Supporting Information. Figure 1s shows the time evolution of number of solvent molecules in the first and second solvation shell. Figure 2s shows a snapshot from the trajectory for the betaine molecule and solvent molecules up to second solvation shell.) Such a large number of solvent molecules requires a large QM box, which automatically brings down the time scale of our simulation. Due to the usually reported behavior of exchange of solvent molecules between the first and second solvation in the liquid state[28,29] the QM water molecule hits the QM boundary which can result in numerical instabilities with subsequent explosion within the simulations. Our aim was to sample more efficiently over the twist angle degrees of freedom which is a much more important effect than the back-polarization effect. Moreover, Rousseau et al. studied[30] the structure of H_3O^+ within a water cluster using both full QM and QM/MM approaches, and they find that the structure of H_3O^+ in water appears to be similar in both models (see Figures 6 and 7 of ref 30). In the present case too, betaine being more polar (or zwitterionic), the QM/MM approach is appropriate to use. Also, if the solute is a less polar molecule use of MM water (for which the charges were optimized to reproduce the dipole moment in bulk water) would have been a problematic issue. However, here since the solute molecule is highly polar the MM water with the TIP3P model is rather appropriate to use.

The CP-QM/MM calculation starts with a quenching run that relaxes the initial structure within the QM/MM setup. Then the temperature scaling run was carried out for 0.5 ps to increase the system temperature to 300 K. Finally, the system was connected to a Nose-Hoover thermostat, and the length of the production run was 60 ps. For a comparative study of OB in the solution phase with the gas phase we also carried out CPMD calculations on a single molecule of OB. The molecular geometry of a single molecule of OB was optimized with the CPMD code,[27] and subsequently, the temperature scaling run and Nose production run were performed. The time scale used for integration of the equation of motion during the scaling and Nose runs was 2 au, and the total time scale for the production run was 5 ps.

2.2. Semiempirical INDO/CIS Calculations. The electronic spectra for single OB and OB−water solute−solvent systems have been calculated using the semiempirical INDO/CIS method[19] as implemented in ZINDO module of the Gaussian03 program.[20] The INDO/CIS calculation has been performed by considering the 10 highest occupied orbitals and 10 lowest virtual orbitals. This method has been successful in reproducing the electronic spectra for E_T30 dye and other structurally similar molecules.[8,13] Also, this method is computationally less demanding and can be applied for few hundreds of configurations including few hundreds of solvent molecules explicitly along with the solute molecule. The electronic spectra for the single OB molecule has been calculated for the configurations obtained from the CPMD trajectories. The electronic spectra have been obtained for a total of 750 configurations separated by 1 fs. For OB in water the electronic spectra have been calculated for a total of 250 configurations separated by 2.5 fs. The solvent molecules ranging between 75 and 95 in number were included

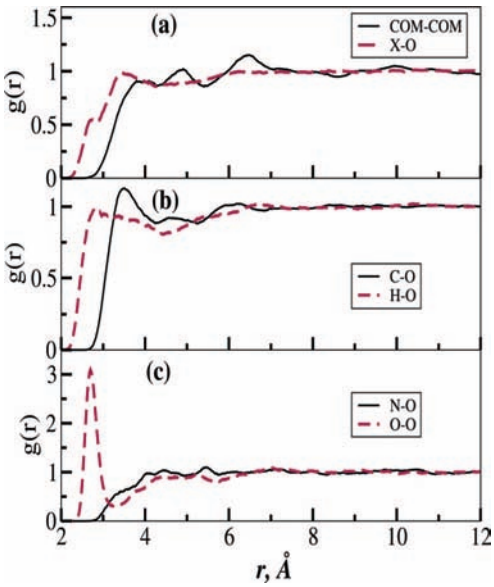

Figure 2. (a) (Solute center-of mass(COM))−(solvent COM) rdf and (solute-all-atoms)−(solvents COM) rdf. (b) (Solute carbon atoms)−(solvent COM) and (solute hydrogen atoms)−(solvent COM) rdfs. (c) (Solute nitrogen atom)−(solvent COM) and (solute oxygen atom)−(solvent COM) rdfs.

along with the OB solute molecule in these calculations. The solvent molecules up to the third solvation shell in the solute−solvent center of mass−center of mass radial distribution function (rdf) were included. The solvation structure of OB in water will be discussed in detail in the later part of the manuscript. Overall, the INDO/CIS calculations for the OB gas phase include 64 valence electrons, while for OB in water they include around 780.

3. Results and Discussions

3.1. Solvation Structure, Molecular Geometry, and Dipole Moment Distribution. Solvent molecules interact with the solute molecule through specific and nonspecific interaction modes. When the solute or solvent molecule has polar groups the interaction mode is naturally site specific. In the OB−water solute solvent system one could expect site-specific interaction modes between the polar carbonyl group and the water molecules. The solvation structure can be conveniently discussed using different solute−solvent rdfs which are constructed from the distances calculated between the solute and solvent sites. In Figure 2 we have shown the center of mass−center of mass rdf ($g_{COM-COM}$) and (solute-all-atoms)−(solvent-COM) rdf (g_{X-O}) along with other atom−atom rdfs. The $g_{COM-COM}$ and g_{X-O} rdfs provide an average picture about how the solvent molecules are arranged around the solute molecule in different solvation shells. For the nonglobular molecules such as the one here, g_{X-O} has been suggested to be better as this function takes into account the solute molecular shape.[31,32] For globular molecules these two functions will be similar in any case. As we see from the $g_{COM-COM}$ rdf the solute molecule has an influence on the solvation structure up to 9 Å, beyond which the bulk density is equal to 1. The C−O, H−O, and N−O atom−atom rdfs suggest a nonspecific interaction with the solvent water molecules, while the strong first peak in the O−O rdf suggests specific interaction of the solvent molecules with the solute oxygen atom.

The molecular geometry of OB is an important aspect to be discussed for a better understanding of the solvatochromic shift.

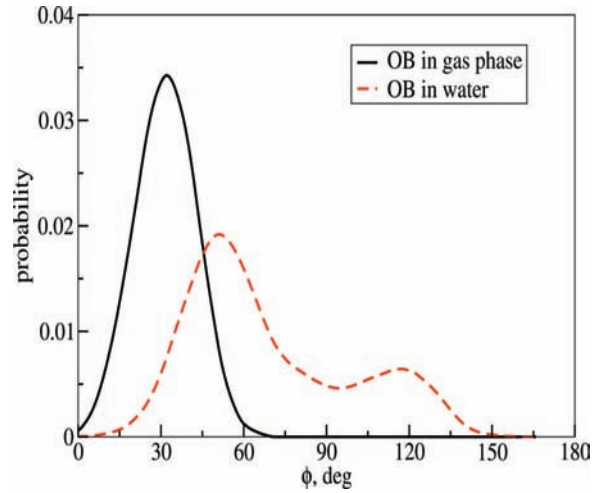

Figure 3. Twist angle distribution function for OB in the gas phase and water. The average twist angle for OB in the gas phase is 30°, while in water it is 55.6°.

Just by mere changing of the twist angle (as defined as ϕ in Figure 1) from 30° to 60° Fonseca et al. predicted a shift of 1530 cm^{-1} for the transition.[13] The twist angle determines how the pyridine and phenoxide rings are arranged relative to each other and hence determines the extent of hyperconjugation. The ab initio electronic structure calculations on a single molecule of OB predicts 30° for the twist angle,[11] while electronic structure calculations with self-consistent reaction field theory suggests that the twist angle increases between 50° and 80° in solvents with the twist angle being reported to be a function of solvent polarity.[11] The twist angle of OB in water has been reported to be 60° based on the free energy perturbation theory calculations.[12] We also investigated the molecular geometry of OB in the gas phase and water. Figure 3 shows the distribution of the twist angle. In both the gas phase and water the amplitude of the twist angle is almost 60°. This clearly suggests that the rigid-body approximation for the OB molecule is inaccurate. For the OB in the gas phase the peak position is around 30°, which is in complete agreement with the previous report on the molecular geometry of OB in the gas phase. In the case of water solvent, the peak position is shifted toward a higher value. Also, in the water solvent the OB molecule shows a conformational transition to another structurally equivalent conformer. The distribution curve displays a shallow barrier around 90°, which shows that the conformer with this twist angle is energetically unfavorable in water solvent. If the simulation is continued long enough one should expect a bimodal distribution curve with equal peak height around either side of $\phi = 90°$. We calculated the average value for the twist angle for OB in water using the distribution curve with $\phi < 90°$, which is 55.6°. The values obtained from ab initio self-consistent reaction field theory calculations[11] (which report a twist angle between 50° and 80°) and free-energy perturbation calculations[12] (which report a twist angle of 60°) are in closer agreement to the value obtained from the present CP-QM/MM calculations.

The OB molecule and other such solvatochromic molecules have been reported to show remarkable solvent shifts in the molecular dipole moments in the ground and excited states. The solvatochromic shift has been attributed to the decrease in the dipole moment of the excited state, which eventually leads to the destabilization in polar solvents, resulting in a negative shift. For the structurally similar 4-(1-pyridinio)phenolate it has been shown that the dipole moment of the ground state (S_0) is 27.1 D in water solvent which decreases to 2.4 D in the excited

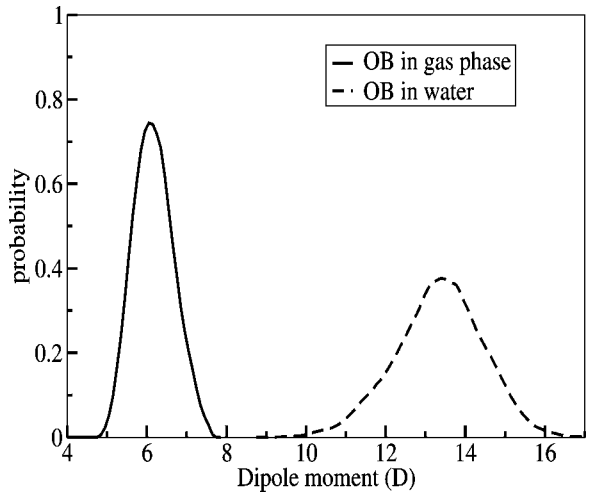

Figure 4. Dipole moment distribution function for OB in the gas phase and water. The average dipole moment for OB in the gas phase is 6.2 Debye, while for OB in water it is 13.3 Debye.

TABLE 1: Average Atomic Charges

system	gas phase	betaine in water
O_1	−0.6663	−0.6833
N_2	0.3528	0.1319
C_3	−0.1115	0.0326
C_4	−0.0830	0.0412
C_5	−0.1234	−0.0110
C_6	−0.0466	0.0118
C_7	−0.0709	−0.0089
C_8	−0.2777	−0.0189
C_9	−0.0787	−0.0368
C_{10}	−0.2034	−0.0846
C_{11}	0.0224	−0.0317
C_{12}	−0.3528	−0.0621
C_{13}	0.6545	−0.0644
H_{14}	0.0885	0.0783
H_{15}	0.0898	0.0464
H_{16}	0.0676	0.0819
H_{17}	0.1315	0.0475
H_{18}	0.1270	0.1245
H_{19}	0.1095	0.1046
H_{20}	0.0900	0.0933
H_{21}	0.1016	0.1110
H_{22}	0.1791	0.0986

state (S_1).[33] In the ground state these molecules are reported to be in a charge-separated form (or a zwitterionic form) in polar solvents and the dipole moment is large, while in the gas phase the charge-separated zwitterionic state cannot be stabilized and the molecule remains in a neutral form. Figure 4 shows the dipole moment distribution for OB in the gas phase and water. The average value of the gas-phase dipole moment is 6.2 D, while the solution-phase value is almost 13.3 D. The experimental gas-phase dipole moment has been reported to be 7.0 D.[13] For OB in water the experimental dipole moment is not known. MP2/cc-pVDZ calculations with the PCM model reports a dipole moment of 11.6 D, while the earlier MP2/6-31G calculations including PCM for the OB molecule with the 60° interring angle (or twist angle) report dipole moments up to 12.3 D.[13] To understand the increased dipole moment of OB in water we calculated the average charges for all atoms in the gas phase and water; the values are given in Table 1. The ESP charges for the OB molecule in the gas phase and D-RESP[16] charges for OB in water are given in the table; both sets of charges are obtained by fitting to the molecular electrostatic potential. In addition, the D-RESP charges include the effect

TABLE 2: Average Charges of Phenoxide and Pyridinium Rings

system	phenoxide	pyridinium
OB in the gas phase	−0.53	0.53
OB in water	−0.73	0.73

of an instantaneous electrostatic field due to the dynamic solvent environment.[16] In both the gas phase and solution phase a significantly larger negative charge is localized over the oxygen atom while a positive charge is localized over the nitrogen atom. A similar trend has been reported by Fonseca et al.[13] from the charges obtained from MP2/6-31G calculations with PCM. As it is difficult to understand the increase in the dipole moment by looking at the atomic charges for OB, we also calculated the total charge on phenoxide and pyridinium rings for OB in the gas phase and water; the values are given in Table 2. One can note that the phenoxide ring has a total negative charge and that the pyridinium ring has a total positive charge. This is in agreement with the zwitterionic model proposed for the OB molecule. An interesting feature is the actual magnitude of the total charge of these two rings in the gas phase and water which increases by almost 0.2 *q*/*e* on going from the gas phase to water, something that has to be attributed to the increase in the dipole moment.

3.2. Solvatochromic Shift. The electronic spectra of OB and other molecules exhibiting large solvatochromic shifts are usually discussed in terms of $\pi-\pi^*$ and $n-\pi^*$ transitions. The analysis of molecular orbitals of OB shows that HOMO, LUMO, and LUMO+1 orbitals are of π character, while the HOMO-1 orbital is n in type. Usually the large solvatochromic shift observed in these molecules is due to the shift in the $n-\pi^*$ excitation due to the solvent. In the case of OB, $\pi-\pi^*$ is the lowest energy excitation and $n-\pi^*$ is the next excitation in energy. From the INDO/CIS calculations (performed for the trajectory obtained from CPMD and CP-QM/MM calculations), we calculated the distribution of excitation energies corresponding to the $\pi-\pi^*$ and $n-\pi^*$ transitions for OB in the gas phase and water. The results are shown in Figure 5 and Table 3. For OB in the gas phase the average energies for the $\pi-\pi^*$ and $n-\pi^*$ excitations are 14 188 and 18 427 cm^{-1}, respectively, from our calculations. The calculated average $\pi-\pi^*$ and $n-\pi^*$ excitation energies for OB in water are 21 636 and 28 773 cm^{-1},

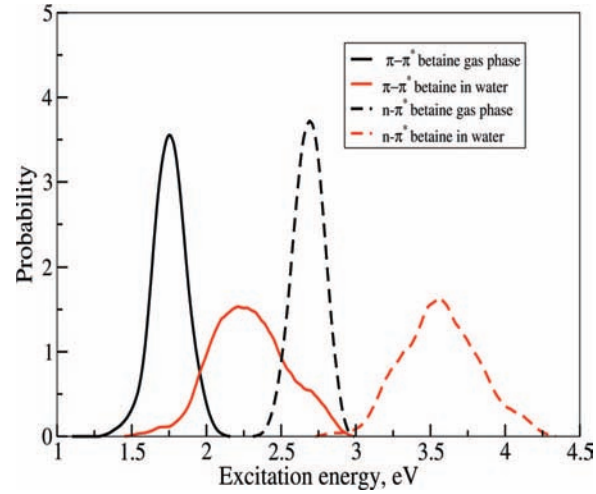

Figure 5. Distribution of $\pi-\pi^*$ and $n-\pi^*$ excitation energies for OB in the gas phase and water. The $\pi-\pi^*$ transition is intraring in nature, while the $n-\pi^*$ transition is associated with the charge-transfer band.

TABLE 3: Average Excitation Energies

system	$\pi-\pi^*$	$n-\pi^*$
betaine in the gas phase	14 188	18 427
betaine in water	21 636	28 773
solvatochromic shift	7448	10 346

respectively. Thus, the calculated solvatochromic shift for OB in water for the $\pi-\pi^*$ transition is 7448 cm^{-1}, while for the $n-\pi^*$ transition the shift is 10 346 cm^{-1}. The experimentally reported λ_{max} values in water and toluene are, respectively, 378 and 529 nm.[8] From these values of absorption maxima the calculated solvatochromic shift for OB from water to toluene solvent is 7552 cm^{-1}. Thus, the actual solvatochromic shift in water from gas phase of OB should be larger than 7552 cm^{-1}. The solvatochromic shift in water compared to the gas phase has been reported to be between 6686 and 9212 cm^{-1} as obtained from interpolation of the absorption maxima data of OB in various solvents.[8] Our combined CP-QM/MM and INDO/CIS calculations predict 10346 cm^{-1} for the solvatochromic shift in water, which is closer to the experimentally calculated maximum value for the solvatochromic shift. The solvatochromic shift reported from the sequential MC-QM calculations is 6360 cm^{-1} , which is in agreement with the minimum value for the experimental solvatochromic shift. We are unable to comment on the predictive ability of the sequential-MC-QM and CP-QM/MM calculations along with the INDO/CIS technique in getting an accurate solvatochromic shift since the experimentally reported solvatochromic shift from vacuum to water has been reported with an error bar as large as $\pm$1266 cm^{-1}.[8] However, the solvatochromic shift reported in the present calculations is as much as 4000 cm^{-1} larger when compared to sequential MC-QM technique. This increase is thus an effect of solute molecular flexibility and the solvent molecular reorganizations adjusted for the instantaneous molecular geometry. Thus, a flexible molecular model for the solute molecule is recommended in the calculations of the solvatochromic shift for OB and other structurally similar molecules.

4. Conclusions

Pyridinium *N*-phenolate betaine dyes play an important role in solution chemistry as indicators of the polarity scale of solvents as these dyes exhibit an intramolecular charge-transfer absorption band that sharply depends on the solvent polarity. In order to understand and predict the solvent effects of the transition shifts as well as other molecular properties we carried out Car−Parrinello CPMD and CP-QM/MM calculations on *o*-betaine in the gas phase and water. These models provide full structural and dynamic flexibility of dye and solvent.

The present calculations clearly show that the OB molecule is highly flexible in both the gas phase and water with a variation in the twist angle by as much as 60°. When compared to the sequential MC-QM calculations the calculated solvatochromic shift increases as much as 4000 cm^{-1}, which has to be attributed to the flexibility of the solute molecule and reorganization of the solvent molecules, which is dependent on the instantaneous solute molecular geometry. Due to the large error bars reported for the experimental solvatochromic shifts we are unable to comment on the accuracy of the predicted solvatochromic shift. However, the present calculations clearly show that inclusion of molecular flexibility contributes as much as 4000 cm^{-1} to the solvatochromic shift and hence recommends incorporation of molecular flexibility for the solvatochromic calculations for OB and other betaine dyes.

The gas-phase dipole moment has been reproduced correctly when compared to experimental values and ab initio electronic structure calculations at the MP2 level. The dipole moment of OB in water increases by as much as two times, which proves the zwitterionic nature in water, in line with the general understanding for similar solvatochromic molecules. Calculation of the total charges of the phenoxide and pyridinium rings in the gas phase and water proves that the charges are more polarized in the water. With the combined CP-QM/MM and INDO/CIS methods we obtain a solvatochromic shift of a little more than 10 000 cm^{-1}, which is in good agreement with the experimentally reported solvatochromic shift values.[8,13] Our work indicates the importance of allowing full structural and dynamic flexibility of dye−solvent systems in predicting their basic solvatochromic properties.

Acknowledgment. N.A.M. acknowledges the Wenner-Gren foundation for financial support. N.A.M. also acknowledges Dr. Prakash Chandra Jha and Dr. Swapan Chakravarthi for useful discussions related to INDO/CIS calculations in the manuscript and Dr. Hakan Hugosson for the use of Gromos and interface codes for CPMD/GROMOS. This work was supported by a grant from the Swedish Infrastructure Committee (SNIC) for the project "Multiphysics Modeling of Molecular Materials", SNIC 023/07-18.

Supporting Information Available: Figure 1s of the Supporting Information shows the time evolution of number of solvent molecules in the first and second solvation shell for betaine. Figure 2s shows a snapshot from the trajectory for the betaine molecule and solvent molecules up to second solvation shell. This material is available free of charge via the Internet at http://pubs.acs.org.

References and Notes

(1) Reichardt, C. *Chem. Rev.* **1994**, *94*, 2319.
(2) Reichardt, C. *Org. Process Res. Dev.* **2007**, *11*, 105.
(3) Reichardt, C.; Che, D.; Heckenkemper, G.; Schafer, G. *Eur. J. Org. Chem.* **2001**, *12*, 2343.
(4) Reichardt, C. *Angew. Chem., Int. Ed.* **1979**, *18*, 98.
(5) Paley, M. S.; Meehan, E. J.; Smith, C. D.; Rosenberger, F. E.; Howard, S. C.; Harris, J. M. *J. Org. Chem.* **1989**, *54*, 3432.
(6) Liptay, W. *Angew. Chem., Int. Ed.* **1969**, *8*, 177.
(7) Mente, S. R.; Maroncelli, M. *J. Phys. Chem. B* **1999**, *103*, 7704.
(8) Gonzalez, D.; Neilands, O.; Rezende, M. C. *J. Chem. Soc., Perkin Trans. 2* **1999**, *1*, 713.
(9) Caricato, M.; Mennucci, B.; Tomasi, J. *J. Phys. Chem. A* **2004**, *108*, 6248.
(10) Bartkowiak, W.; Lipinski, J. *J. Phys. Chem. A* **1998**, *102*, 5236.
(11) Caricato, M.; Mennucci, B.; Tomasi, J. *Mol. Phys.* **2006**, *104*, 875.
(12) Hernandes, M. Z.; Longo, R.; Coutinho, K.; Canuto, S. *Phys. Chem. Chem. Phys.* **2004**, *6*, 2088.
(13) Fonseca, T. L.; Coutinho, K.; Canuto, S. *Chem. Phys.* **2008**, *349*, 109.
(14) Andreoni, W.; Curioni, A. *Parallel Comput.* **2000**, *26*, 819.
(15) Carloni, P.; Rothlisberger, U.; Parrinello, M. *Acc. Chem. Res.* **2002**, *35*, 455.
(16) Laio, A.; VandeVondele, J.; Rothlisberger, U. *J. Phys. Chem. B* **2002**, *106*, 7300.
(17) Laio, A.; VandeVondele, J.; Rothlisberger, U. *J. Chem. Phys.* **2002**, *116*, 6941.
(18) Car, R.; Parrinello, M. *Phys. Rev. Lett.* **1985**, *55*, 2471.
(19) Ridley, J.; Zerner, M. C. *Theor. Chim. Acta.* **1973**, *32*, 111.
(20) Frish, M. J. ; Schlegel, H. B.; Scuseria, G. E.; Robb, M. A.; Cheeseman, J. R.; Montgomery, J. A., Jr.; Vreven, T.; Kudin, K. N.; Burant, J. C.; Millam, J. M.; Iyengar, S. S.; Tomasi, J.; Barone, V.; Mennucci, B.; Cossi, M.; Scalmani, G.; Rega, N.; Petersson, G. A.; Nakatsuji, H.; Hada, M.; Ehara, M.; Toyota, K.; Fukuda, R.; Hasegawa, J.; Ishida, M.; Nakajima, T.; Honda, Y.; Kitao, O.; Nakai, H.; Klene, M.; Li, X.; Knox, J. E.; Hratchian, H. P.; Cross, J. B.; Adamo, C.; Jaramillo, J.; Gomperts, R.; Stratmann, R. E.; Yazyev, O.; Austin, A. J.; Cammi, R.; Pomelli, C.; Ochterski, J. W.; Ayala, P. Y.; Morokuma, K.; Voth, G. A.; Salvador, P.; Dannenberg, J. J.; Zakrzewski, V. G.; Dapprich, S.; Daniels, A. D.; Strain,

M. C.; Farkas, O.; Malick, D. K.; Rabuck, A. D.; Raghavachari, K.; Foresman, J. B.; Ortiz, J. V.; Cui, Q.; Baboul, A. G.; Clifford, S.; Cioslowski, J.; Stefanov, B. B.; Liu, G.; Liashenko, A.; Piskorz, P.; Komaromi, I.; Martin, R. L.; Fox, D. J.; Keith, T.; Al-Laham, M. A.; Peng, C. Y.; Nanayakkara, A.; Challacombe, M.; Gill, P. M. W.; Johnson, B.; Chen, W.; Wong, M. W.; Gonzalez, C.; Pople, J. A. *Gaussian 03*, Rev. B.05; Gaussian, Inc.: Pittsburgh, PA, 2003.

(21) Wang, J.; Wolf, R. M.; Caldwell, J. W.; Kollman, P. A.; Case, D. A. *J. Comput. Chem.* **2004**, *25* (9), 1157.

(22) Jorgensen, W. L.; Chandrasekhar, J.; Madura, J. D.; Impey, R. W.; Klein, M. L. *J. Chem. Phys.* **1983**, *79*, 926.

(23) Case, D. A.; Cheatham T. E.; Simmerling, C. L.; Wang, J.; Duke, R. E.; Luo, R.; Merz, K. M.; Wang, B.; Pearlman, D. A.; Crowley, M.; Brozell, S.; Tsui, V.; Gohlke, H.; Mongan, J.; Hornak, V.; Cui, G.; Beroza, P.; Schafmeister, C.; Caldwell, J. W.; Ross, W. S.; Kollman, P. A. *AMBER8*; University of California: San Francisco, CA, 2004.

(24) Becke, A. D. *Phys. Rev. A* **1988**, *38*, 3098.

(25) Lee, C.; Yang, W.; Parr, R. C. *Phys. Rev. B* **1988**, *37*, 785.

(26) Trouiller, N.; Martins, J. L. *Phys. Rev. B* **1991**, *43*, 1993.

(27) Hutter, J.; Parrinello, M.; Marx, D.; Focher, P.; Tuckerman, M.; Andreoni, W.; Curioni, A.; Fois, E.; Roetlisberger, U.; Giannozzi, P.; Deutsch, T.; Alavi, A.; Sebastiani, D.; Laio, A.; VandeVondele, J.; Seitsonen, A.; Billeter, S. Computer code CPMD, version 3.11; IBM Corp. and MPI-FKF: Stuttgart, 1990−2002.

(28) Pal, S. K.; Zewail, A. H. *Chem. Rev.* **2004**, *104* (4), 2099.

(29) Pal, S. K.; Peon, J.; Bagchi, B.; Zewail, A. H. *J. Phys. Chem. B* **2002**, *106* (48), 12376.

(30) Rousseau, R.; Kleinschmidt, V.; Schmitt, U. W.; Marx, D. *Phys. Chem. Chem. Phys.* **2004**, *6*, 1848.

(31) Georg, H. C.; Coutinho, K.; Canuto, S. *J. Chem. Phys.* **2007**, *126*, 034507−1.

(32) Canuto, S.; Coutinho, K.; Trzesniak, D. *Adv. Quantum Chem.* **2002**, *41*, 161.

(33) Ishida, T.; Rossky, P. *J. Phys. Chem. B* **2008**, *112*, 11353.

JP8097395